TECHNICAL UNIVERSITY OF CLUJ-NAPOCA

ACTA TECHNICA NAPOCENSIS

Series: Applied Mathematics, Mechanics, and Engineering
Vol. 69, Issue II, June, 2026

FUNCTIONAL REQUIREMENTS AND THEIR FULFILMENT FOR A ROTARY FRICTION WELDING DEVICE

Mihai BOCA, Margareta COTEAȚĂ, Oana DODUN, Andrei-Marius MIHALACHE, Laurențiu SLĂTINEANU

Abstract: *Rotary friction welding is a process of joining two components made of metallic or plastic materials, due to the heat generated by rotating one component relative to the other and pressing one part against the other, while one of them remains in a fixed position. From a practical perspective, it is of interest to evaluate the magnitude of the axial force of pressing one part against the other. The problem addressed here is the design of a device to evaluate the effects of various factors on the magnitude of the axial force in rotary friction welding. The gradual outline of a constructive solution was possible by applying some principles of axiomatic design. To obtain additional information about the rotary friction welding process, the welding of two aluminium rods was considered. Additional verification of some hypotheses was possible using the finite element method.*

Key words: *rotary friction welding, axial force, axiomatic design, functional requirements, design parameters, lathe adaptive device.*

1. INTRODUCTION

The welding process is a manufacturing process that joins two parts, whether metallic or plastic, using heat and, optionally, applied force as local pressure, with or without a filler material, to achieve a non-destructive assembly. The welding processes offer several advantages, including low-cost production, the ability to achieve high-complexity assemblies, and efficient production times. The importance of welding lies in obtaining assemblies with the highest mechanical properties, which are used in various engineering domains, including aerospace, automotive, naval, electrical, tooling, construction, and others. [1, 2].

Depending on the change in the thermal phase, the welding process can be divided into two types. One is characterised by applying high temperatures to the materials to be joined, with the addition of filler material, and is called *fusion welding*. The other category uses a temperature close to the material's melting point and applies pressure to supposedly welded materials to achieve perfect contact between them. This process is known as *pressure welding*.

Rotary friction welding (RFW) is considered a pressure welding process. It is a solid-state welding process that uses frictional heat to join two metallic parts. It is considered a solid-state welding process, and it is assumed that frictional heat generates the necessary temperature for welding. It should be noted that the joint materials must be of the same type and have the same chemical structure and physical properties [1, 2].

To date, some research has been conducted on various aspects of rotary friction welding. Thus, in one of the studies, the authors explore the design and functionality of a laboratory-scale rotary friction welding setup for joining dissimilar materials, specifically aluminium bronze Ca104 to austenitic stainless steel AISI316 [3]. The research results demonstrate the successful application of the setup, showing changes in hardness along the weld interface and evidence of metallic diffusion between dissimilar materials. The study highlights the

Received: 28.04.26; **Similaritie**s: 07.05.26: **Reviewed**:28.04. /28.04.26: **Accepted** 08.06.26.

potential of a bespoke machine for nuclear energy applications, emphasising its ability to produce high-integrity joints with short weld times and without the need for expensive industrial-grade equipment. Additionally, it is essential to note that the process is performed on a drilling machine, with the two parts aligned along the machine's vertical axis.

Other research focuses on optimising the RFW parameters. There are studies of dissimilar joints in geological exploration drill pipes made of AISI 1330 and AISI 4340 steels [4]. The study concludes that specific microstructural changes are crucial for achieving high joint strength, offering valuable insights for improving the welding process. The optimised parameters result in strong, durable joints that can withstand the demanding conditions of geological exploration. The research highlights the importance of precise control of welding parameters to achieve the desired mechanical properties and reliability in joints between dissimilar materials. However, it does not provide details about the axial force values.

Other studies, conducted as reviews, discuss the fundamental principles of RFW, the conversion of kinetic energy into heat energy to create high-quality welds [1]. Some key welding parameters, such as friction force, forge force, friction pressure, and forge pressure, are examined [5], with few details about the force-effective values.

In the article by Parmar [2], a comprehensive review of the RFW process is presented. The review provides a general introduction to friction welding, including the various types of friction welding processes (linear, rotary, inertia, and friction stir welding), as well as its benefits, such as cost-effectiveness, high production rates, and strong welds. The paper addresses the working principles, experimental setups, and objectives of the review of existing literature on friction welding. Besides those described previously, some studies present mechanical properties, microstructural analyses, and the optimisation of welding parameters for different materials. The review concludes that friction welding offers significant advantages over conventional welding methods, particularly in terms of weld quality and material efficiency.

In another study [6], the researchers investigated the RFW process for two different grades of carbon steel (Ck22 and St50). The study examines the impact of rotational speed and welding time on the mechanical properties and microstructure of the welds. The optimal process parameters were a rotational speed of 1400 rpm and a welding time of 8 seconds. The research includes detailed microstructural analysis, describes tensile and microhardness tests, and highlights fractography images. The results indicate that RFW can produce high-quality welds with minimal defects, making it well-suited for joining low-cost structural alloys. The study also highlights other environmental benefits, including reduced emissions and lower energy consumption, compared to traditional welding methods. In this case, specific values for the rotation speed and welding time are applied.

Another study [7] explores the impact of various RFW parameters on the joint strength of different alloys. The paper discusses the history, evolution, and fundamentals of RFW, including the key components and types of RFW processes. It highlights the advantages of the RFW process, such as high joint strength, minimal material waste, and the ability to join dissimilar materials. The review also examines the economic benefits and environmental impact of RFW compared with conventional welding methods. The study has demonstrated the effect of welding parameters, including rotational speed, axial pressure, and friction process time, on the mechanical properties of welded joints. The paper concludes that RFW is a cost-effective and environmentally friendly welding technique suitable for various industrial applications.

None of the aforementioned authors has presented information on measuring the required pressure force and applying it to evaluate the necessary force for the materials being joined. Additionally, no information is available on the specific axial force values to be applied. Additionally, the pressing force can influence the shape and size of the crystalline grains formed in the joint area. Based on this consideration, the value obtained for the mechanical resistance characteristics of the resulting assembly is determined.

Regarding other possible devices for measuring axial force in the RFW process, a study by Zuluaga-Posada et al. [8] describes a custom-built axial-force-measuring device integrated into a CNC system for friction stir welding (FSW), a process closely related to RFW. This device can capture force values that align with expected trends, validating its effectiveness. However, this device is adapted for the FSW process, as is the other device presented in the study [3].

Other recent research in the field of solid-state joining emphasises the optimisation of friction-based processes for high-performance materials, particularly aluminium and copper. An analysis of FSW specifically for aluminium alloys [9] highlights the ongoing importance of this technique in modern manufacturing.

The challenge of joining dissimilar materials is a central theme, with a comparative review [10] focusing on enhancing joint strength between aluminium and copper alloys through rotary friction welding (RFW). This investigation is supported by experimental and numerical studies [11] that demonstrate how varying the friction time directly influences plastic deformation and the overall structural integrity of the Al-Cu interface. Furthermore, detailed metallographic and mechanical characterisations of continuous drive friction welding [12] provide a deeper.

Additionally, the study explores the potential application of axiomatic design principles to develop a device that measures the force generated during the welding process. Several aspects of determining the force required to be applied to one of the workpieces in an RFW process were also addressed, specifically for the rotary friction welding of two 3 mm-diameter aluminium rods. Finite Element Analysis (FEA) was utilised to obtain additional information concerning the temperature distribution within the contact zone between the two workpieces to be joined.

2. ROTARY FRICTION WELDING

As presented above, friction welding is a pressure welding process that relies on generating friction between the two components, thereby raising the temperature in the contact area to achieve a welded assembly. The principle of the method is to maintain one of the two components to be welded in a fixed position while allowing the other to rotate relative to the first. Next, to achieve the welded joint, a pressing force is applied to generate heat. The rotation movement is stopped when the phenomenon of pushing out, or expelling the excess material, occurs. *The main steps* of the process include the following [13]:

1. Contact and rotation: one workpiece is clamped and rotated at high speed, while the other remains stationary;
2. Heat generation: the rotating part is pressed against the stationary one, causing frictional heat to build up at the interface.
3. Plastic deformation: as the temperature increases, the material at the interface softens without reaching its melting point;
4. Forge welding: once the optimal temperature is reached, the rotation stops abruptly, and axial force is applied, forging the materials together.

At the end of the process, the welded joint is left to cool, resulting in a strong metallurgical bond.

In certain situations, the welding process enables the repair of machine parts, such as shafts or axles, that have fractured during operation.

Rotary friction welding involves several key output parameters that present interest in technical and economic directions. These parameters are crucial for assessing the efficiency, quality, and cost-effectiveness of the welding process. *The technical output parameters* obtained are:

1. Tensile strength that indicates the maximum stress the welded joint can support before breaking when stretched or pulled;
2. Impact toughness that measures the welded joint's ability to absorb energy and also to resist fracture under impact;
3. The hardness factor that reflects the welded joint's resistance to deformation or indentation;
4. The microstructure that highlights the grain structure and phase distribution within the welded joint, influencing its mechanical properties;

5. Heat-Affected Zone (HAZ) that could emphasise the area of the base material affected by the welding heat, but not melted. The HAZ properties are vital for the overall strength and durability of the weld.

These parameters are crucial in evaluating the quality and performance of welding joints in various applications.

As economic output parameters, it can be highlighted:

1. Cycle time that is the total time required to complete one welding cycle, including heating, forging, and cooling. Shorter cycle times can increase production rates and reduce costs;

2. Material utilisation that represents the efficiency of materials used in welding. Higher material utilisation reduces waste and lowers costs;

3. The welding process requires energy. Lower energy consumption leads to cost savings and improved sustainability;

4. Operational costs include expenses related to labour, maintenance, and consumables. Efficient processes with lower operational costs are economically beneficial.

Several technical and operational factors affect the magnitude of the axial force in friction welding. These factors can be grouped into categories, each of which significantly impacts the axial force values. Some of these parameters could also be considered technical factors or input parameters:

1. Rotational speed: higher rotational speeds can increase the temperature at the welding interface, thereby reducing the magnitude of the required axial force;

2. Axial feed rate: higher feed rates can increase the axial force;

3. Workpiece geometry: the shape and size of the welding face of the workpiece affect heat generation and material flow;

4. Material properties involve the mechanical and thermal properties of the welded materials, which influence the magnitude of the required axial force.

As operational factors, with a considerable impact on the axial force developed, can be considered:

1. Contact pressure: the pressure applied between the workpieces affects heat generation and, consequently, the magnitude of the axial force;

2. Initial temperature: higher initial temperatures of the workpieces can reduce the magnitude of the required axial force due to decreased material resistance;

3. Lubrication: the lubricants can reduce friction and, thus, the required axial force.

3. FUNCTIONAL REQUIREMENTS FOR A DEVICE, FOR STUDYING THE INFLUENCE OF DIFFERENT FACTORS ON THE AXIAL FORCE AT RFW

The research aimed to design an RFW device that enables experimental study of how various process input factors affect the magnitude of the axial force required to initiate welding.

The axiomatic design method could be used to identify the functional requirements that the force-measuring device must satisfy. This design methodology contributes to a systematic approach to the design activities [14]. Thus, the method enables the analysis and design of equipment for the development of rotary friction welding technology. Professor Nam Pyo Suh proposed the theory of axiomatic design to encourage creativity and to systematically search for a constructive solution to a problem, thereby minimising the interactive process of finding a solution [14]. The applicability of the methodology spans a range of fields, including engineering, economics, waste management, and medical applications, among others.

Axiomatic design can be considered a methodology to enhance the quality and efficiency of design processes. The four key domains defined in axiomatic design are [14]:

1. Customer Domain: identifies the needs of the end-user.
2. Functional Domain: defines the Functional Requirements (FRs) that the product must meet to satisfy those needs.
3. Physical Domain: identifies the Design Parameters (DPs) that fulfil the specified FRs.
4. Process Domain: establishes the manufacturing variables required to produce the DPs.

The functional domain defines the product's or process's *functional requirements*. These requirements define the functions that the product should perform to meet the user's needs. The domain involves clearly outlining the objectives and goals that the product must achieve. For instance, in the case considered, functional requirements might include, among others, measuring the magnitude of the pressure force, which depends on the weld diameter. At the same time, the physical domain focuses on a physical solution that fits the functional requirements specified in the functional domain. This involves determining the structure and physical components needed to accomplish the desired functions. The domain translates functional requirements into technical specifications and engineering solutions.

In axiomatic design, the zero-order functional requirement (FR0) is defined as the system's or product's primary purpose. It is a fundamental requirement that enables the system to function correctly. FR0 is expressed straightforwardly and clearly to capture the project's main objective. Additionally, the FR0 should be concise and transparent, as it reflects the core function the system or product must perform. For the study considered, the FR0 requirement is to obtain functional equipment to measure the axial force required for optimal welding conditions when using RFW.

In axiomatic design, the design parameter (DP0) that fulfils the zero-order functional requirement (FR0) is identified as the key variable defining the design solution. DP0 should be directly linked to FR0 and provide a clear, effective means of meeting the primary functional requirement.

DP0 should be articulated in a way that clearly shows how the design solution will meet the zero-order functional requirement. This step is essential for ensuring the design is practical and meets user needs. As described, the considered DP0 goal is equipment capable of ensuring the conditions for measuring the axial force developed during the joining process.

In axiomatic design, first-order functional requirements (FR1) are derived directly from the zero-order functional requirement (FR0). These requirements are detailed, specific, and oriented, and will break FR0 into smaller, manageable components that must be fulfilled to achieve the primary goal: measuring the pressure force.

These first-order functional requirements help elaborate and clarify the zero-order functional requirements, making the design and implementation process more straightforward.

First-order design parameters (DPs) are the key variables that define design solutions to meet first-order functional requirements (FRs). These parameters are crucial for effectively addressing the detailed functional requirements.

4. DEVELOPING A SOLUTION USING SOME PRINCIPLES OF THE AXIOMATIC DESIGN FOR THE DEVICE

Considering the functional requirement and design parameter of zero-order, the functional requirements and first-order design parameters might be:

FR1: Ensure the variation of the magnitude of the pressing force; DP1: Compressible Spring;

FR2: Ensure the change of the pressing force magnitude; DP2: Spring compression screw;

FR3: Ensure the measurement of the pressing force. DP3: Subsystem using a dial gauge;

FR4: Ensure the locating and clamping of the fixed part to be welded; DP4: Drill chuck;

FR5: FR5: Ensure the placement of the force generation and measurement components; DP5: Bushing-type part;

FR6: Ensure the locating and clamping of the bushing-type part; DP6: Parallelepiped-shaped part;

FR7: Ensure the locating and clamping of the welding part to be rotated; DP7: Universal lathe chuck

FR8: Ensure the rotation of the welding part; DP8: strung universal.

The previously proposed decision matrix for the functional requirements (FR) and design parameters (DP) is presented in Table 1.

The analysis of the decision matrix in Table 1 reveals that a lower-triangular matrix was obtained, corresponding to a decoupled design. Such a design is considered acceptable, as it ensures compliance with the independence requirement of the functional requirements, in accordance with the first axiom of axiomatic design.

5. PROPOSED SOLUTION FOR AXIAL FORCE MEASUREMENT DEVICE IN ROTARY FRICTION WELDING

The device proposed for measuring the force required to achieve jointing between two cylindrical workpieces is intended to study the rotary welding process. It was also intended for use on a horizontal universal lathe (Fig. 1). The device consists of a base bushing 1 that holds a spring 2. One end of the spring presses against the front surface of a screw 3, which is threaded into the base bushing. This screw includes a cylindrical area to guide the spring. The other end of the spring presses against part 4, which also has a cylindrical guiding zone for the spring. Part 4 is threaded into an inner bushing 5, which transmits the force generated during the rotary friction welding of two cylindrical rods (6 and 7) considered the parts to be welded. The rod 6 is located and clamped in chuck A, which is added to part 4. Its front surface is pressed against the front surface of rod 7, which is held in the chuck (B) of the lathe.

The axial force measurement could be performed using spring compression. The pressure applied during welding will cause the inner bushing to move. In this way, a screw inserted into the inner bushing carries a flat element 9 that contacts a probe 10 of a dial gauge D. The dial gauge indicates the spring's compression length, thereby correlating it with the applied force. In this way, it is possible to obtain data on the required welding pressure.

Forward, a rectangular part 8 is welded to the base bushing 1, enabling the device to be mounted onto one of the four slots of a lathe tool holder C. Component 11 serves as the mounting element that sustains the dial gouge D.

In conclusion, the force correlates directly with the spring's compression, and the spring

Table 1

Decision matrix

Desing parameters / Functional requirements	DP1: Spring	DP2: Spring compression screw	DP3: Subsystem using a dial gauge	DP4.: Drill chuck	DP5: Bushing type part	DP6: Parallelepiped part	DP7: Universal lathe chuck	DP8: Universal lathe
FR1: Ensure the variation of the magnitude of the pressing force	X							
FR2: Ensure the change of the pressing force magnitude		X						
FR3: Ensure the measurement of the pressing force			X					
FR4: Ensure the locating and clamping of the fixed part to be welded				X				
FR5: Ensure the placement of the force generation and measurement components	X	X	X	X	X			
FR6: Ensure the locating and clamping of the bushing-type part	X	X	X	X	X	X		
FR7: Ensure the locating and clamping of the welding part is rotated							X	
FR8: Ensure the rotation of the welding part	X	X	X	X	X	X	X	X

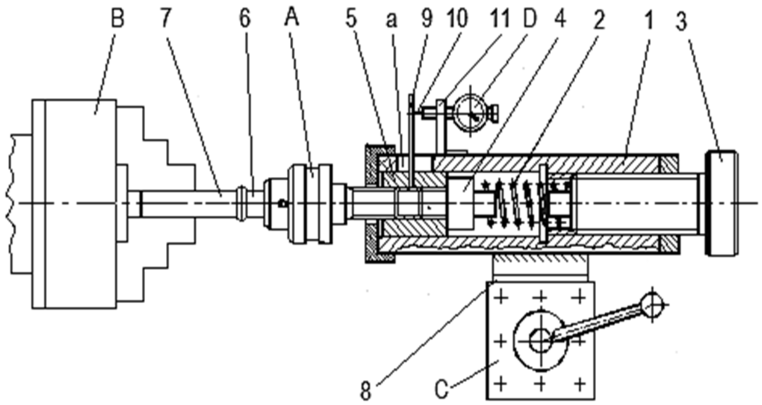

Fig. 1. The schematic design of the RSW force-measuring device.

could be calibrated to determine the welding pressure. This means that the measurement method is performed indirectly by using the spring compression value.

Several significant advantages of the device's solution need to be highlighted. One of them involves measuring and evaluating the magnitude of the pressure force required to achieve a welding joint.

This condition is achieved because the device is equipped with a calibrated spring and a dial gauge, which enable the measurement and control of the force applied during welding. In this way, the device will provide information on the magnitude of the pressure force required to be applied to the flat ends of two parts, one of which is clamped in the lathe tool holder, to meet the welding process requirements.

The device is designed for use on a universal lathe, providing a solution for various machining environments. Its compatibility with tool holders adds versatility.

6. THE FORCE REQUIRED FOR FRICTION WELDING OF TWO ALUMINUM RODS

In the case of the device proposed for use on a universal lathe for the friction welding of aluminium rods, the force required to be exerted by the stationary rod on the rotating rod must be provided by compressing the helical spring within the device's assembly. To determine the magnitude of this force, a pressure of p = 20-50 MPa is considered, which is generally recommended for the friction welding of aluminium. If we consider the friction welding of aluminium rods with a diameter of d = 3 mm, the contact surface area between the two rods will be:

$$A = \frac{\pi d^2}{4} = 7.07 \cdot 10^{-6}\ m^2. \qquad (1)$$

Assuming a pressure value of p = 30 MPa, the magnitude of the force F required to be exerted by the spring within the device can be estimated as follows:

$$F = pA = 30 \cdot 10^6 \cdot 7.07 \cdot 10^{-6} \approx 212\ \text{N}. \qquad (2)$$

Taking into account a friction coefficient μ=0.4 and a rod cross-sectional radius R= 1.5mm, the friction torque M can be calculated as follows:

$$M = \frac{2}{3}\mu F R = 0.66 \cdot 212 \cdot 0.0015 = 0.0848\ \text{N}\cdot\text{m}. \qquad (3)$$

Assuming that the rotating rod rotates at a speed of n = 1200 rpm, the angular velocity ω of the rod's rotation will correspond to the following relationship:

$$\omega = \frac{2\pi n}{60} = \frac{2 \cdot \pi \cdot 1200}{60} = 125\frac{rad}{s}. \qquad (4)$$

The peripheral velocity v corresponding to the angular velocity ω is:

$$v = \omega R = 125 \cdot 0.0015 = 0.187\frac{m}{s}. \qquad (5)$$

Knowing the peripheral velocity v, the power generated by friction can be estimated as:

$$\text{P} = \mu \cdot \text{F} \cdot \text{v} = 0.4 \cdot 212 \cdot 0.187 = 15.8\ \text{W}. \qquad (6)$$

The heat flux at the interface between the two rods will correspond to the following relationship:

$$q = \frac{P}{A} = \frac{15.8}{7.07 \cdot 10^{-6}} = 2.23 \cdot 10^6\ \text{W/m}^2. \qquad (7)$$

For the melting temperature of aluminium, Tm=660°C, a welding temperature of Tw≈0.7·Tm=462°C is estimated. If an ambient temperature of 20°C is considered, a temperature increase of ΔT=462-20=442°C will be required to reach the plasticity state of the aluminium. Assuming the end of the rod is brought to a plastic state over a thickness of h≈1 mm, the volume of this zone will be: $V=A \cdot h=7.07 \cdot 10^{-6} \cdot 0.001=7.07 \cdot 10^{-9}$ mm^3.

Taking into account an aluminium density of ρ=2700 kg/m3, the amount of material brought to a plastic state will be:

$$m=\rho \cdot V=2700 \cdot 7.07 \cdot 10^{-9} = 0.000019 \text{ kg}. \quad (8)$$

Knowing the specific heat of aluminium, c = 900 J/(kg·K), the energy required for welding the rods can now be estimated:

$$Q=m \cdot c \cdot \Delta T=0.000019 \cdot 900 \cdot 442=7.55 \text{ J}. \quad (9)$$

The time required for welding is determined as the ratio between the energy and the power required to develop the welding process of the rods:

$$t=\frac{Q}{P}=\frac{7.55}{15.8}=0.47\ s. \quad (10)$$

Allowing for thermal energy losses of approximately 50-70%, the time required to develop the welding process is aprox at 1-2 s.

7. FINITE ELEMENT METHOD SIMULATION OF THE THERMAL FIELD IN THE WELDING AREA

The design of a rotary friction welding device, approached in this research through the framework of Axiomatic Design, necessitates a thorough understanding of the thermomechanical environment at the weld interface. In rotary friction welding, heat is generated exclusively through viscous dissipation and dry Coulomb friction between the mating surfaces, one of which rotates at a prescribed angular velocity. At the same time, the other is held stationary under an applied axial compressive force. The resulting temperature field governs the plasticisation of the material in the weld zone, the width of the thermally affected region, the residual stress state after cooling and, critically, the mechanical performance of the joint.

Consequently, a reliable prediction of the thermal field represents a functional requirement in itself, directly linked to the design parameters of the axial force measurement device proposed in this work, such as the temperature distribution that determines the expected thermal expansion of structural components, the operating range of the measurement chain, and the selection of appropriate sensor technologies.

Finite Element Method (FEM) simulation may be selected as a predictive tool due to its ability to handle the complex, spatially non-uniform heat source characteristic of rotary friction welding, as well as the temperature-dependent material properties and multiple simultaneous heat transfer mechanisms that govern this process. The numerical model is constructed and solved within the ANSYS environment.

The thermal analysis of the friction welding zone was conducted using a Transient Thermal analysis system within ANSYS Workbench (version 2024 R1 researcher license), accessed through the Mechanical application. This module solves the general unsteady heat conduction equation in its weak form over the discretised domain, making it appropriate for capturing the evolution of the temperature field during the friction phase. A steady-state thermal analysis would be inadequate in this context because the heat source is transient by nature: e.g., the friction phase lasts a finite, controlled duration, after which the rotation ceases; the axial upsetting force is then applied, and the thermal field subsequently decays by conduction and surface heat loss.

It should be noted that a fully coupled thermomechanical analysis, employing the Coupled Field Transient module in ANSYS, would be the most physically complete approach, as it would simultaneously account for frictional heat generation, plastic deformation work, and the material's mechanical softening. However, such an analysis engages significantly greater computational cost and requires validated flow stress models over a wide temperature range. For the purpose of characterising the thermal field as a design input for the measurement device, the uncoupled transient thermal approach is considered sufficiently accurate, provided the heat generation is prescribed as a time-dependent boundary condition at the interface.

The geometry of the weldment, two coaxial cylindrical rods pressed end-to-end, exhibits continuous rotational symmetry about the common longitudinal axis. Exploiting this symmetry, the three-dimensional problem was reduced to an equivalent two-dimensional axisymmetric model, in which the solution domain is a meridional half-plane defined by the radial coordinate r and the axial coordinate z, with the axis of symmetry lying along $r = 0$. The physical interpretation of this reduction is that neither the temperature field nor the material properties vary with the circumferential coordinate θ, an assumption that is valid during the steady-rotation phase and is a research-accepted simplification for the thermal analysis of rotary friction welding of cylindrical specimens.

The asymmetric formulation was implemented in ANSYS by activating the corresponding option in the geometry and meshing settings, which was achieved by defining a 2D planar geometry and selecting Axisymmetric as the 2D behaviour in the geometry details panel. The origin of the coordinate system was placed at the centre of the weld interface, so that the two halves of the assembly, corresponding to the rotating and stationary workpieces, occupy the regions. $z > 0$ and $z < 0$ respectively, with the weld plane coinciding with $z = 0$.

The thermal response of the model is governed primarily by three temperature-dependent material properties, as follows: thermal conductivity. $\lambda(T)$, specific heat capacity $c_{\mathrm{p}}(T)$, and mass density ρ. For metallic workpieces commonly joined by rotary friction welding, including low-carbon structural steels and engineering aluminium alloys, these properties exhibit non-negligible temperature dependence, particularly in the range between ambient temperature and the solid or incipient melting temperature of the alloy. Incorporating this dependence is essential for accurate prediction of the peak temperature and the spatial extent of the thermally affected zone. Temperature-dependent material data were entered in the Engineering Data workspace by defining tabular values of each property as a function of temperature. These data were sourced from standardised handbooks. Isotropic behaviour was assumed in the thermal conductivity tensor, which is appropriate for wrought metals without strong crystallographic texture in the axial–radial plane. The authors acknowledge the limitations of using handbook-sourced data, which may be incomplete or erroneous.

The primary heat source in rotary friction welding is the frictional power dissipated at the contact interface between the two workpieces. In the classical formulation, the local heat flux is generated per unit area at a radial position. r on the interface is given by:

$$q(r) = \mu \cdot p \cdot v(r) = \mu \cdot p \cdot \omega \cdot r, \quad (11)$$

where μ is the coefficient of friction at the interface, p is the contact pressure, ω is the angular velocity of the rotating workpiece in rad/s, and r is the local radial coordinate. The μ can be temperature-dependent and is generally an uncertain parameter in friction welding models, and the p is assumed to be uniform in the simplest formulation and to be distributed according to elastic or elastic–plastic contact theory in more advanced models. The equation shows that the frictional heat flux is linearly proportional to the radius: the outer periphery of the interface generates substantially more heat per unit area than the central region, whereas the axis of symmetry contributes no heat.

In ANSYS Workbench, this spatially varying heat flux is applied as a surface boundary condition on the interface plane ($z = 0$) of the model. The spatial distribution expressed by Equation (3) can be incorporated in simplified analyses by approximating the flux as uniform and equal to the area-averaged value, as in the present case. The total power input to the interface is obtained by integrating Equation (12) over the interface area. In this expression R is the outer radius of the workpiece cross-section. This total power is a useful quantity for verifying the model's energy balance.

$$Q_{\mathrm{total}} = \int_0^{\mathrm{R}} q(r) \cdot 2\pi r \, dr = (2\pi/3) \cdot \mu \cdot p \cdot \omega \cdot R^3 \quad (12)$$

The heat flux boundary condition is applied throughout the friction phase τ_f, after which it is set to zero to simulate the termination of rotation. Our calculation gives an approximate value of 59 W for a 3-mm-diameter rod.

The lateral cylindrical surface of each workpiece, as well as the free end face of each rod, loses heat to the surrounding environment primarily by natural convection. In ANSYS Mechanical, this is applied as a convection boundary condition characterised by a heat transfer coefficient, h and an ambient reference temperature. For natural convection of a vertical or horizontal cylinder in air at moderate temperatures, the heat transfer coefficient typically ranges from 5–25 W/(m²·K), depending on the surface orientation, characteristic length, and temperature difference. In many friction welding simulations reported in the literature, a representative value of $h \approx$ 10–15 W/(m²·K) is adopted as a reasonable estimate for free convection in air. Radiative heat loss may also be included for surfaces at elevated temperatures using the surface emissivity, ε appropriate for the oxidation state of the material, but they are generally relevant above approximately 300–400°C and were not used in the present case, which is considered an ideal simplified one.

No thermal boundary condition is applied explicitly along the axis of symmetry ($r = 0$) because the asymmetric formulation automatically enforces zero radial heat flux ($\partial T/\partial r = 0$) at $r = 0$ as a natural boundary condition, which is physically correct, by symmetry, no heat flows across the axis. A uniform initial temperature equal to the ambient temperature T_0, commonly of about 20–25°C, is applied throughout the entire domain at $t = 0$ via the Initial Temperature setting in the Analysis Settings branch.

The quality and spatial resolution of the finite element mesh are critical determinants of the accuracy of the predicted temperature field, particularly near the weld interface, where steep thermal gradients are expected. In the present 2D model, the mesh was generated using quadrilateral elements with quadratic shape functions, such as Quad8, which are quads with 8 nodes preferred over linear triangular elements for thermal problems because they introduce less numerical diffusion and achieve higher accuracy for a given node count.

A non-uniform mesh was generated across the solution domain, with high element density concentrated near the weld interface and the axis of symmetry, where the temperature gradients are steepest.

The element size in the immediate weld zone was set to a fraction of the expected thermal penetration depth, estimated a priori from the thermal diffusivity. $\alpha = \lambda/(\rho \cdot c_\mathrm{p})$ and the friction phase duration τ_f as $\delta \approx \sqrt{(\alpha \cdot \tau_f)}$, to ensure the numerical discretisation does not smooth out the actual spatial gradient. Away from the interface, the mesh gets progressively coarsened using a bias factor, reducing the total element count without sacrificing accuracy in the regions of interest. Mesh independence was verified by comparing the peak temperature at the weld interface and the temperatures at representative monitoring points obtained from successively refined meshes (as shown in Figure

Table 2

Boundary conditions applied in ANSYS.

Boundary / Location	**Condition Type**	**Parameter / Value**	**Notes**
Weld interface (z = 0)	Prescribed heat flux	$q(r) = \mu \cdot p \cdot \omega \cdot r \approx 12.5$ MW/m²	Active during the friction phase only and zero during the forge and cooling phases
Lateral surfaces	Convection	h ≈ 10–15 W/(m²·K); $T_{ambient}$ = 20–25°C	Natural convection in air; radiation optionally added for T > 300°C
Free end faces	Convection (or adiabatic)	Same as lateral surfaces	Adiabatic if clamped in an insulating fixture
Axis of symmetry (r = 0)	Zero radial flux (automatic)	$\partial T/\partial r = 0$	Enforced implicitly by the axisymmetric formulation
Full domain at t = 0	Initial temperature	T_0 = 20–25°C	Uniform; matches ambient shop-floor conditions

2). The solution was considered mesh-converged when the change in peak temperature between two successive refinement levels fell below 1% of the peak value.

The transient heat conduction equation was integrated in time using the implicit time integration tool, which is unconditionally stable and therefore imposes no restriction on the time step size from a stability standpoint. Nevertheless, the time step must be chosen small enough to resolve the temporal evolution of the temperature field with adequate accuracy, particularly during the friction phase when the heat flux changes most rapidly. An automatic time-stepping strategy was employed, in which the solver adjusts the time step within user-prescribed minimum and maximum bounds based on the estimated rate of change of the solution.

The simulation was divided into load steps corresponding to the main phases of the welding cycle. One is dedicated to the friction phase, characterised by the prescribed interfacial heat flux and duration. τ_f, and another to the cooling phase, during which the heat flux is removed and the temperature field decays by conduction and convective surface loss. The results depicted in Figure 2 correspond to the thermal field at a specific instant at the end of the friction phase, as evidenced by the persistence of the localised hot zone at the weld interface.

The computed temperature distribution presented in Figure 2 reveals the complex, highly non-uniform thermal field that develops in the weld zone during the friction phase of the rotary friction welding cycle.

The maximum temperature attained in the model, approximately 370–375°C as indicated by the dark red region at the top of the jet colour scale, is located at or very near the axis of symmetry ($r \approx 0$) and at the weld interface plane ($z \approx 0$).

This spatial location, as expressed by Equation (11), the frictional heat flux is proportional to the local sliding velocity, which itself is proportional to r, and therefore vanishes at the axis and reaches its maximum at the outer

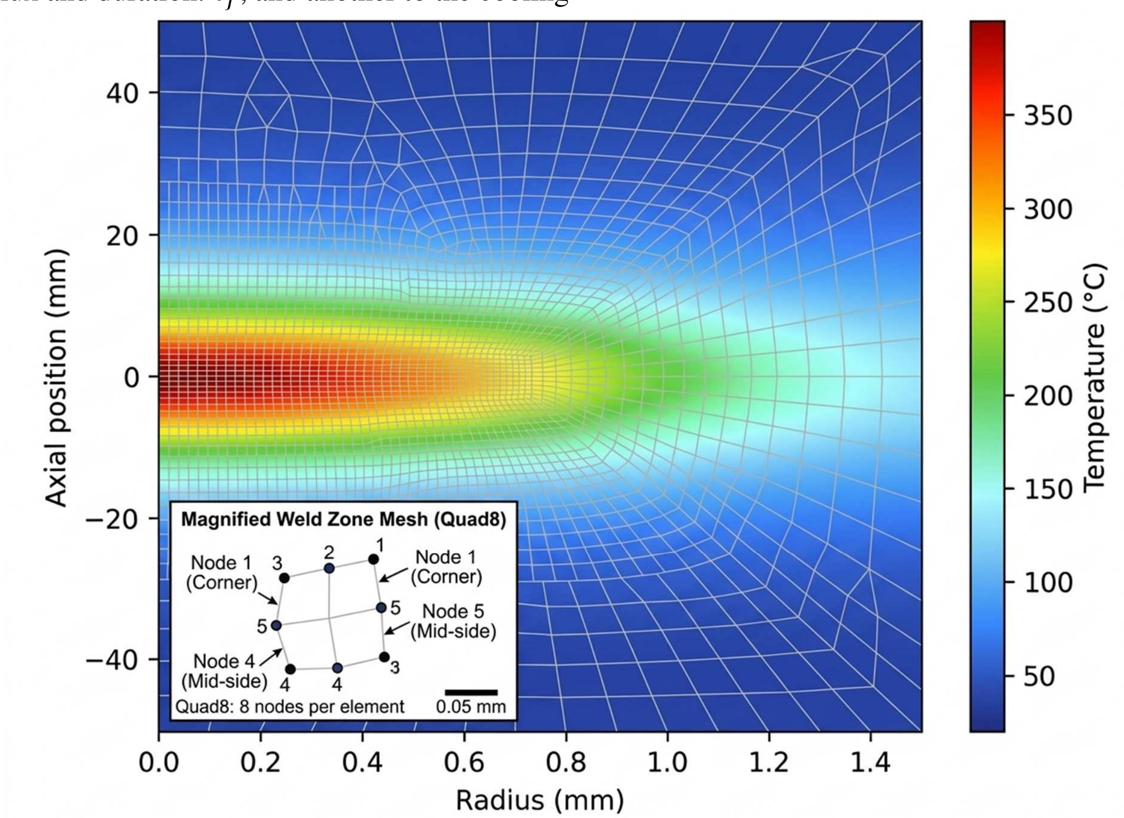

Fig. 2. Computed temperature distribution in the meridional half-plane of the rotary friction welding assembly with mesh elements.

periphery.

The observation of the highest temperature at the axis is therefore a consequence of heat conduction from the periphery toward the axis during the course of the friction phase, rather than direct heat generation at $r = 0$.

In other words, the thermal diffusion process redistributes the energy generated preferentially at large radii, and the relatively small cross-sectional area of the central region, combined with the absence of heat removal at $r = 0$, results in a local temperature maximum at the axis. This behaviour is consistent with findings reported in the open literature for friction welding of cylindrical specimens, and underscores the importance of transient simulation.

The authors state that a simplistic steady-state argument based solely on the heat generation distribution would incorrectly predict the highest temperature at the outer radius.

Moving along the axial direction away from the interface, the temperature decreases monotonically from the peak value toward the ambient background temperature. The gradient is steepest immediately adjacent to the interface and becomes progressively shallower as one moves further from the weld plane. From Figure 2, the isothermal contours, which appear as elongated, horizontally symmetric lobes on either side of $z = 0$, suggest that the region where the temperature exceeds approximately 100°C extends by approximately 20 mm on each side of the interface. This defines the thermal heat-affected zone (HAZ) in the axial direction, within which the thermal cycle may be sufficient to alter the material's microstructure, mechanical properties, or residual stress state.

The symmetry of the thermal field about $z = 0$, that is, the identical temperature distributions in the two halves of the weldment, is consistent with the assumption of identical materials and identical thermal boundary conditions on both sides of the interface. In practice, minor asymmetries may arise from differences in fixture contact conditions or surface finishes, but these are secondary effects for design-level analysis.

In the radial direction, at the level of the weld interface ($z = 0$), the temperature decreases from its peak value at $r = 0$ to the ambient background as r increases toward the outer boundary at $r = 1.5$ mm. The transition visible in Figure 2 is relatively abrupt near the axis; the dark red region of approximately 340–375°C is confined to a very narrow band at $r \lesssim 0.1$ mm, transitioning through orange and yellow of approximately 250–340°C over $r \approx 0.1 - 0.3$ mm, through green of approximately 180–250°C over $r \approx 0.3 - 0.8$ mm, and reaching cyan and finally deep blue near-ambient, below 100°C, beyond $r \approx 1.2 - 1.5$ mm. This steep radial gradient reflects the highly localised nature of frictional heating in small-diameter specimens and the relatively high thermal conductivity of metallic materials, which limits the lateral spread of the thermal plume during the short duration of the friction phase.

From the standpoint of the axial force measurement device, this steep radial gradient implies that any temperature-sensitive element of the measurement chain, such as a strain gauge, a piezoelectric transducer, or a load cell, should be located at a radial distance sufficient to remain below its rated operating temperature. The present results suggest that, for the specific process parameters and material combination modelled, components positioned at a radial distance greater than approximately 1.5 mm from the workpiece axis and at an axial distance greater than approximately 30 mm from the weld interface would experience temperatures only marginally above ambient, a useful design constraint for sensor placement.

The overall morphology of the thermal field, an elongated, ellipsoidal hot zone centred on the weld interface with its major axis aligned with the rotation axis, is characteristic of the diffusion-dominated heat transfer regime in friction welding of cylindrical specimens. The aspect ratio of the heated zone, with axial extent much greater than radial extent, reflects the geometry of the problem. The heat generated at the small circular interface is free to diffuse along the full length of the rod. In contrast, radial diffusion is constrained by the outer boundary, which acts as a partial heat sink via convection.

The peak temperature of approximately 375°C, if confirmed to be below the recrystallisation temperature of the material being welded, would suggest that the friction phase is operating in a regime of solid-state bonding driven by thermally activated diffusion and plastic deformation of the asperities, rather than by localised melting. This is consistent with the fundamental characteristic of rotary friction welding as a solid-state process. Conversely, if the material has a low melting point or if the process parameters produce temperatures exceeding the solidus, a thin flash layer of molten metal may form at the interface, a condition not modelled in the present thermal-only simulation but addressable by introducing a phase-change model in an extended future analysis.

From the perspective of the axiomatic design methodology applied in the current research, the thermal field simulation constitutes a direct fulfilment of the functional requirement that the weld zone temperature must remain below the material's bonding threshold while simultaneously ensuring that the heat-affected zone does not extend to the measurement components of the axial force device. The simulation results confirm that, under the modelled conditions, the thermal gradient is sufficiently steep in both the radial and axial directions to permit the placement of temperature-sensitive measurement elements at distances that are practically achievable within the device's mechanical envelope. The authors consider this finding to support the feasibility of the proposed design and to provide quantitative bounds on the standoff distances and thermal shielding requirements for the measurement chain.

The authors further acknowledge the limitations of the present study, which was treated as an ideal setup, and recommend treating the results with caution.

8. CONCLUSIONS

Rotary friction welding (RFW) is a solid-state welding technique where one component is rotated against another under axial pressure. The friction between the surfaces generates heat, causing the material to become plasticised and form a permanent bond. Research in specialised literature indicates that RFW is effective for welding similar and dissimilar materials. It provides a narrow heat-affected zone and maintains high molecular integrity. The method is widely used in automotive, aerospace, and underwater engineering industries. The objective of the research presented in this article was to design a device adaptable to a universal lathe to assess the influence of various input factors on the resulting output parameters in the rotary friction welding (RFW) process. The design challenges were addressed by applying principles of axiomatic design. To determine the magnitude of the force required to be exerted by the stationary component on the rotating part during the RFW process, conditions corresponding to the welding of two 3 mm diameter aluminium rods were considered. This approach also enabled an evaluation of the welding process duration. Furthermore, the Finite Element Method (FEM) facilitated visualisation of the temperature distribution within the contact zone between the two rods. The primary limitations of the results stem from the use of approximate values for certain RFW-specific variables and the adoption of specific assumptions regarding material behaviour during welding. Future research will focus on the physical fabrication of the device and testing it under various rotary friction welding conditions.

9. REFERENCES

[1] Makvana, V., Shah, M., Mahant, J., Choudhary, A. M., Savalia, D., *Rotational friction welding a review paper,* International Journal of Research and Analytical Reviews, E-ISSN 2348-1269, 2020.

[2] Parmar, V. R., Patel, J., Surani, P., *A Review Paper on Rotary Friction Welding*, Journal of Emerging Technologies and Innovative Research, ISSN-2349-5162, 2022.

[3] Dellepiane, M., Da Silva, L., Toumpis, A., *Design and development of a bespoke rotary friction-welding machine in exploration of joining dissimilar materials for nuclear applications*, J. Manuf. Mater. Process, https://doi.org/10.3390/jmmp9010027, 2025.

[4] Rangasamy, S., Kamalamurthy, S., Ponnusamy, S., Bellamkonda, N.P., Visvalingam, B., *Optimisation of mechanical properties of rotary friction welding parameters of low alloy steel tubes using design of experiments concept*, International Journal on Interactive Design and Manufacturing - Springer, https://doi.org/10.1007/s12008-023-01214-x, 2023

[5] Isaeva, A., Priymak, E., Atamashkin, A., Kirilenko, A., *Optimisation of rotary friction welding parameters for dissimilar joints of exploration drill pipes*, The International Journal of Advanced Manufacturing Technology, pp. 5325–5337, https://doi.org/10.1007/s00170-023-11382-5, 2023.
[6] Savitharoja, P., Kumar, M. D., Noorullah, D., *A study review on rotary friction welding,* International Journal of Innovative Research in Technology, ISSN: 2349-6002, 2023.
[7] Nabi, A.-A., Mojtahedi, M., Choghaie, E.-H., *Effect of process parameters on the rotary friction welding of CK22-ST50 carbon steels*, Metallurgical and Materials Transactions, pp. 740-751, https://doi.org/10.1007/s11661-024-07678-0, 2025.
[8] Gilbert, T. G., Aravind Raj, R., Aradhak, S., Joshan, G., Nevin, N., *Effect of Rotary Friction Welding Parameters on the Different Alloys' Joint Strength: A Review*, International Journal of Innovative Science and Research Technology, Vol. 9, Issue 2, ISSN: 2456-2165, 2024.
[9] Feddal, I., Chairi, M., Di Bella, G. *Analysis of Friction Stir Welding of Aluminum Alloys*, Metals 15, 532, https://doi.org/10.3390/met15050532, 2025.
[10] Ariyansah, R., Prabowo, A.R., Muhayat, N., Nugroho, B.A., Triyono, T., *Comparative Review of Rotary Friction Welding Between Aluminium and Copper Alloys for Enhanced Joint Strength*, Eng. Proc. 84, 92. https://doi.org/10.3390/engproc2025084092, 2025.
[11] Ratkovi´c, N., Arsi´c, D., Nikoli´c, R.R., Deli´c, M., Jovanovi´c Peši´c, Ž., Mandi´c, V., Pastorkova, J., *Experimental and Numerical Analysis of Rotary Friction Welding for Al-Cu Joints: Effects of Friction Time on Plastic Deformation and Joint Integrity*, Materials. https://doi.org/10.3390/ma18091932, 2025.
[12] Sauter L., Werz M., Weihe S., *Continuous drive friction welding of commercial pure aluminum to copper: Metallographic and mechanical characterization of various cross-sections*, Journal of Advanced Joining Processes, ISSN 2666-3309, https://doi.org/10.1016/j.jajp.2025.100342, 2025.
[13] Zaluaga-Posada, M., Hoyos, E., Montoya, Y., *Performance evaluation of a novel force measuring device for Friction Stir Welding (FSW) of aluminium alloys,* DYNA, pp. 150-155,https://doi.org/10.15446/dyna.v86n210.70359, 2019.
[14] Suh, N. P., *Axiomatic Design-Advances and Applications*, Oxford University Press, ISBN 0-19-513466-4, New York, 2001.

Cerințe funcționale și îndeplinirea lor în cazul unui dispozitiv de sudare prin frecare rotativă

Sudarea prin frecare rotativă este un proces de îmbinare a două componente din materiale metalice sau plastice, datorită căldurii generate prin rotirea uneia dintre componente față de cealaltă și prin apăsarea uneia dintre ele pe cealaltă, în timp ce una dintre acestea rămâne în poziție fixă. Dintr-o perspectivă practică, prezintă interes evaluarea mărimii forței axiale de apăsare a unei piese asupra celeilalte. Problema abordată într-un astfel de context este reprezentată de conceperea unui dispozitiv care să permită evaluarea influenței diferiților factori asupra mărimii forței axiale în sudarea prin frecare rotativă. Conturarea treptată a unei soluții constructive a fost posibilă prin aplicarea unor principii ale proiectării axiomatice. Pentru obținerea unor informații suplimentare referitoare la procesul de sudare prin frecare rotativă, a fost luată în considerare sudarea a două tije din aluminiu. O verificare suplimentară a unor ipoteze a fost posibilă prin utilizarea metodei elementului finit.

Mihai BOCA, PhD., Lecturer, "Gheorghe Asachi" Technical University of Iasi, Machine Manufacturing Technology Department, mihai.boca@academic.tuiasi.ro, 0040743195870.
Margareta COTEAȚĂ, PhD., Associate Professor, "Gheorghe Asachi" Technical University of Iasi, Machine Manufacturing Technology Department, margareta.coteata@academic.tuiasi.ro, 0040752141598.
Oana DODUN, PhD., Professor, Gheorghe Asachi Technical University of Iasi, Machine Manufacturing Technology Department, oana.dodun-des-perrieres@academic.tuiasi.ro, 0040747144604.
Andrei-Marius MIHALACHE, PhD., Associate Professor, "Gheorghe Asachi" Technical University of Iasi, Machine Manufacturing Technology Department, marius-andrei.mihalache@academic.tuiasi.ro, 004075356715.
Laurențiu SLĂTINEANU, PhD., "Gheorghe Asachi" Technical University of Iasi, Machine Manufacturing Technology Department, laurentiu.slatineanu@academic.tuiasi.ro, 0040723718675.